

Elevated plasma and urinary erythritol is a biomarker of excess simple carbohydrate intake in mice

Semira R. Ortiz¹ and Martha S. Field¹

From the ¹Division of Nutritional Sciences, Cornell University, Ithaca, NY 14853, USA

Corresponding author: Martha S. Field, mas246@cornell.edu, (607) 255-6081

113 Savage Hall, Division of Nutritional Sciences, Ithaca, NY 14853, USA

Author last names: Ortiz, Field

Running title: Plasma/urinary erythritol is a biomarker of simple carbohydrate intake

Funding sources: This work is supported by Hatch Federal Capacity Funds [grant no. 7000420] from the USDA National Institute of Food and Agriculture to MSF. This work was supported by the Education and Workforce Development Predoctoral Fellowship [grant no. 2021-67034-35110/project accession no. 1026400] from the USDA National Institute of Food and Agriculture to SRO.

Declarations of interest: None

Abbreviations: ADH1: alcohol dehydrogenase 1; DIO: diet-induced obesity; G6PD: glucose-6-phosphate dehydrogenase; HFD: high-fat diet; IPGTT: intraperitoneal glucose tolerance test; KO: knockout; LFD: low-fat diet; PPP: pentose phosphate pathway; SORD: sorbitol dehydrogenase; TKT: transketolase; WT: wildtype.

1 **Abstract**

2 **Background:** Elevated serum erythritol is a predictive biomarker of diabetes and cardiovascular
3 incidence and complications. Erythritol is synthesized endogenously from glucose, but little is
4 known regarding the origin of elevated circulating erythritol *in vivo*.

5 **Objective:** *In vitro* evidence indicates that intracellular erythritol is elevated by high-glucose cell
6 culture conditions and that final step of erythritol synthesis is catalyzed by the enzymes SORD
7 and ADH1. The purpose of this study was to determine if dietary intake and/or diet-induced
8 obesity (DIO) affect erythritol synthesis in mice, and if this relationship is modified by loss of
9 the enzymes SORD or ADH1.

10 **Methods:** First, 8-week-old, male *Sord*^{+/+}, *Sord*^{-/-}, *Adh1*^{+/+}, and *Adh1*^{-/-} mice were fed either low-
11 fat diet (LFD) with 10% fat-derived calories or DIO high-fat diet (HFD) with 60% fat-derived
12 calories for 8 weeks. Plasma and tissue erythritol were measured using GC-MS. Second, wild-
13 type 8-week-old C57BL/6J mice were fed LFD or HFD with plain drinking water or 30%
14 sucrose water for 8 weeks. Blood glucose and plasma and urinary erythritol were measured in
15 non-fasted and fasted samples. Tissue erythritol was measured following sacrifice. Finally,
16 *Sord*^{+/+} and *Sord*^{-/-} mice were fed LFD with 30% sucrose water for two weeks, then non-fasted
17 plasma, urine, and tissue erythritol were quantified.

18 **Results:** Plasma and tissue erythritol were not impacted by loss of *Sord* or *Adh1* on LFD or
19 HFD. In wild-type mice, consumption of 30% sucrose water significantly elevated plasma and
20 urinary erythritol on both LFD and HFD compared to plain water. *Sord* genotype did not affect
21 plasma or urinary erythritol in response to sucrose feeding, but *Sord*^{-/-} mice had reduced kidney
22 erythritol content compared to wildtype littermates in response to sucrose.

23 **Conclusions:** Sucrose intake, not high-fat diet, elevates erythritol synthesis and excretion in
24 mice. Loss of ADH1 or SORD does not significantly impact erythritol levels in mice.

25 **Keywords:** Erythritol, pentose phosphate pathway, sucrose, glucose, obesity, sorbitol
26 dehydrogenase, alcohol dehydrogenase

27

28 **Introduction**

29 Cardiometabolic diseases (such as diabetes, heart attack, and non-alcoholic fatty liver
30 disease) begin to develop decades before clinical markers are apparent. The discovery and
31 characterization of new biomarkers can facilitate early detection, and thus early intervention to
32 prevent chronic disease progression. Serum erythritol is one biomarker with the potential to
33 detect the metabolic dysregulation that precedes cardiometabolic diseases (1). Prospective cohort
34 studies indicate that serum erythritol is elevated decades before the incidence of Type 2 Diabetes
35 Mellitus and cardiovascular disease (2–8). Elevated erythritol has been consistently identified as
36 a biomarker not only for future disease incidence, but also for worse outcomes in diagnosed
37 patients (9–11).

38 Erythritol is a polyol traditionally thought of as a nonnutritive sweetener but was also
39 recently found to be synthesized by humans through the pentose phosphate pathway (PPP) (4).
40 Labelled erythritol appeared in plasma following the ingestion of universally labelled ¹³C-
41 glucose, indicating that erythritol was synthesized from glucose (4). Ex vivo analysis of whole
42 blood further indicated that erythritol is produced from erythrose-4-phosphate through the non-
43 oxidative PPP (4). Little is known regarding the physiological role of erythritol in mammals.

44 Two mammalian enzymes have been identified that convert erythrose to erythritol:
45 alcohol dehydrogenase 1 (ADH1) and sorbitol dehydrogenase (SORD) (12). ADH1 and SORD
46 are homologous dehydrogenases (12). SORD is a strong candidate to catalyze erythritol
47 synthesis in mammals. Knockdown of *SORD* in cell culture models reduces erythritol synthesis
48 by 40% in high glucose conditions (12). In mice, tissues containing the most endogenous
49 erythritol (the liver and kidney) are also the metabolic tissues in which SORD expression are
50 highest (13). The impact of ADH1 expression on erythritol synthesis has not been explored. In

51 human cells, erythritol synthesis also exhibits a dose-response to the amount of glucose provided
52 in culture media, suggesting that erythritol may respond to nutrient excess (14).

53 There have been no studies on the factors that contribute to endogenous erythritol
54 synthesis *in vivo* in mammals. The purpose of this work was to determine the role of the enzymes
55 SORD and ADH1 in erythritol synthesis and how erythritol levels are impacted by diet *in vivo*.
56 This is the first study to report that erythritol synthesis and excretion is elevated in response to a
57 high-sucrose diet.

58

59 **Methods**

60 **Generation of the *Sord*^{-/-} mice**

61 We used crispr.mit.edu to select the guide RNA sequence with minimal off-target effects,
62 targeting exon 4 of *Sord* (guide sequence: 5'-AGAAGAAGATAGTCGCGCTC-3'). Template
63 DNA was generated by PCR using the forward primer: 5'-
64 GAAATTAATACGACTCACTATAGGAGAAGAAGATAGTCGGCGTCGTTTTAGAGCTA
65 GAAATAGC-3' and reverse primer: 5'-
66 GCACCGACTCGGTGCCACTTTTTCAAGTTGATAACGGACTAGCCTTATTTAACTTGC
67 TATTTCTAGCTCTAAAAC-3'. Two identical 50 µL reactions were prepared consisting of 25
68 µL GoTaq DNA Polymerase (Promega), 0.5 µL forward primer, 0.5 µL reverse primer, and 24
69 µL nuclease-free water. DNA was denatured at 94°C for 5 minutes, followed by 40 cycles of 30
70 second denaturation at 94°C, 30 second annealing at 58°C, 20 second extension at 72°C. Final
71 elongation was performed at 72°C for 5 minutes. PCR product was pooled, and the DNA
72 amplicon was purified using the MinElute PCR Purification Kit (Qiagen) per manufacturer's
73 instructions. DNA quality was checked by NanoDrop and agarose gel.

74 *In vitro* transcription was completed using the MegaShortscript T7 Transcription kit
75 (ThermoFisher) according to the manufacturer's protocol. Transcription incubation was
76 performed overnight at 37°C in a dry incubator. RNA was then purified using the MEGAClear
77 Transcription Clean-Up Kit (ThermoFisher) per manufacturer protocol. RNA quantity was
78 determined by Qubit. Quality was verified by denaturing 1 µL RNA, 1 µL formaldehyde loading
79 dye (Ambion), and 8 µL nuclease free water in a thermocycler at 65°C for 10 minutes. The
80 denatured RNA was run on an agarose gel to check for the presence of a single sgRNA species.
81 RNA was stored at -80°C until microinjection.

82 Embryos were isolated from 15 C57BL/6J donor females. Pure sgRNA and Cas9 mRNA
83 were microinjected into the pronucleus and cytoplasm of 203 1 cell embryos. Of the 1 cell
84 embryos, 174 advanced to the 2-cell stage and were transferred equally to 6 pseudo-pregnant
85 recipient female mice. 50 founder (F0) pups were born.

86 DNA was isolated from tail snips with the High Pure PCR Template Preparation Kit
87 (Roche) per the manufacturer's instructions. The 400 base pair region surrounding the sgRNA
88 target was then amplified by PCR (forward primer: 5'-CCCAGAGAGGAGGCTGTAGA-3';
89 reverse primer: 5'-AAAGGCCTCCCAGGGGTTAT-3') with GoTaq DNA Polymerase
90 (Promega). The resulting PCR product was cloned into the pCR 4-TOPO vector using the TOPO
91 TA Cloning Kit for Sequencing (Invitrogen). Briefly, 4 µL PCR product, 1 µL Salt Solution, and
92 1 µL pCR 4-TOPO Vector were combined and incubated for 5 minutes at room temperature. The
93 TOPO cloning reaction was then transformed into One Shot TOP10 Chemically Competent *E.*
94 *coli* and plated on 50 µg/mL kanamycin LB plates. After incubation overnight at 37°C, 4
95 colonies per mouse were picked and cultured overnight in 4 mL LB medium with 50 µg/mL
96 kanamycin. Vector DNA was purified using the Zyppy Plasmid Miniprep Kit (Zymo Research)

97 according to the manufacturer's protocol. Plasmids were analyzed by Sanger sequencing to
98 detect mutations in the *Sord* gene (M13 Forward (-20) primer: 5'-GTAAAACGACGGCCAG -
99 3').

100 F0 males with a confirmed mutation in the *Sord* gene were mated with C57BL/6J females
101 to obtain heterozygous F1 pups. *Sord* deletion was confirmed by a 50% reduction in liver SORD
102 protein in F1 *Sord*^{+/-} mice, measured by western blot analysis. *Sord*^{+/-} male and female mice were
103 mated to produce *Sord*^{+/+} (wildtype, WT) and *Sord*^{-/-} (knockout, KO) mice.

104 **Animal dietary treatments and tissue collection**

105 All mice were maintained under specific-pathogen-free conditions in accordance with
106 standard of use protocols and animal welfare regulations. All study protocols were approved by
107 the Institutional Animal Care and Use Committee of Cornell University. All mice were housed
108 individually in environmentally controlled conditions (12 hour light/12 hour dark cycle). *Adh1*
109 mice have been previously described and were backcrossed 10 generations to a C57Bl/6J
110 background (15). At 8 weeks of age, male *Sord*^{+/+}, *Sord*^{-/-}, *Adh1*^{+/+}, and *Adh1*^{-/-} mice were
111 randomly assigned to one of two diets: low-fat diet (LFD) with 10% fat-derived calories or diet-
112 induced obese (DIO) high-fat diet (HFD) with 60% fat-derived calories. Diets were based on the
113 AIN-93G Purified Rodent Diet (Dyets Inc., Bethlehem PA, DYET#'s 104783 and 103651). Diet
114 compositions are provided in **Supplementary Table 1 (LFD) and 2 (HFD)**. Food and water
115 were provided *ad libitum* for 8 weeks. Food intake and body weight were measured twice
116 weekly. Food intake was determined by subtracting the weight of food remaining in the hopper
117 from the weight of food that was supplied. Body composition was measured by NMR after 2, 5,
118 and 8 weeks of treatment using a Bruker Minispec LF65 according to the manufacturer's
119 protocols. Body composition measurements included free fluid, lean, and fat mass.

120 To measure the impact of sugar intake on erythritol synthesis, additional 8-week-old male
121 C57BL/6J mice were randomly assigned to one of four diets for eight weeks. Diets included low-
122 fat diet with plain drinking water (LFD), high-fat diet with plain drinking water (HFD), LFD
123 with 30% sucrose in drinking water (LFD+30% Sucrose) and HFD with 30% sucrose in drinking
124 water (HFD+30% Sucrose). Body weight, food intake, and body composition were assessed as
125 described above. Caloric intake from water was calculated from milliliters of 30% sucrose
126 consumed.

127 Following dietary treatment, all mice were killed by carbon dioxide asphyxiation and
128 cervical dislocation. Plasma and tissues (adipose, liver, kidney, quadriceps) were harvested and
129 snap-frozen in liquid nitrogen, followed by storage at -80°C for use in later applications.

130 **Intraperitoneal glucose tolerance testing**

131 Mice were fasted for 5 hours prior to intraperitoneal glucose tolerance testing (IPGTT).
132 Mice were injected intraperitoneally with 1.5 mg glucose/g body mass. Blood glucose was
133 measured at 15, 30, 60, 90, and 120 minutes following glucose injection. All blood samples were
134 collected from a single nick in the tail vein. Blood glucose was measured via a drop of blood
135 applied to a hand-held glucometer (OneTouch). The area under the curve was calculated using
136 Prism software.

137 **Collection of plasma and urine**

138 Blood was collected from a nick in the tail vein into an EDTA-coated microvette tube
139 (Sarstedt). Whole blood was centrifuged for 10 minutes at 2,000 x g and 4C, then plasma was
140 transferred to an Eppendorf tube and stored at -80C for later analysis of plasma metabolites.
141 Urine samples were collected as previously described (16). Fasted samples were collected
142 following a 5-hour daytime fast.

143 **Isolation and measurement of polar metabolites by GC-MS**

144 Polar metabolites were isolated from mouse plasma, tissues, and urine as described
145 previously (13). Urine was diluted 1 part to 2 parts Milli-Q water prior to isolation with
146 extraction fluid. To account for urine concentration, creatinine was measured using the
147 Creatinine (urinary) Colorimetric Assay Kit per the manufacturer's protocol (Cayman
148 Chemical).

149 Dried metabolites were then derivatized and analyzed by GC-MS as previously described
150 (13). In SIM mode, mass spectra of m/z 217, m/z 307, and m/z 320 were acquired from 8-9 min,
151 m/z 218, m/z 320, and m/z 423 were acquired from 10-11 min, and m/z 319, m/z 331, and m/z
152 421 were acquired from 12-13 minutes. Erythritol, sorbitol, and ¹³C₁-ribitol peaks were selected
153 from GC-MS chromatograms based on the retention time of their respective standards. Absolute
154 intensities of erythritol (m/z 217), sorbitol (m/z 319), and ¹³C₁-ribitol (m/z 218) were recorded.
155 The ratio of the absolute intensity of erythritol or sorbitol to that of ribitol (relative intensity) was
156 used to determine plasma erythritol concentration. Tissue samples were normalized by dividing
157 the relative metabolite intensity by tissue mass in grams. Urine samples were normalized by
158 dividing the relative metabolite intensity by the sample creatinine concentration.

159 **Western blot analysis**

160 Frozen tissue samples were homogenized in lysis buffer containing 15% NaCl, 5 mM
161 EDTA, pH 8, 1% Triton X100, 10 mM Tris-Cl, 5 mM DTT, and 10 µl/mL protease inhibitor
162 cocktail (Sigma Aldrich). Protein concentration was determined by Lowry assay (17). Equal
163 amounts of protein (25-50ug) were denatured by heating with 6X Laemelli buffer for 5-10 min at
164 95 °C. Samples were then loaded onto a 10% SDS-PAGE gel and electrophoresed. Protein was
165 transferred by electrophoresis to an Immobilon-P PVDF membrane (Millipore Corp.).

166 The membrane was blocked in 5% non-fat milk overnight at 4°C, then incubated with
167 primary antibodies for 1 hour at room temperature. Primary antibodies included sorbitol
168 dehydrogenase (1:2,000, Proteintech), alcohol dehydrogenase 1, lamin B1, transketolase, and
169 alpha-tubulin (1:1,000, Cell Signaling Technology). Secondary anti-rabbit antibody (1:100,000,
170 ThermoFisher) was applied to the membrane and incubated for 1 hour at room temperature.
171 Protein was detected using a Protein Simple FluorChem E with Clarity Western ECL Substrate
172 (Bio-Rad). Band intensity was measured using ImageJ (NIH).

173 **Statistical analysis**

174 All statistical analyses were conducted using GraphPad Prism 9 (Graphpad Software Inc).
175 No blinding to treatment group was performed. Differences between two groups (sucrose pilot
176 and sucrose exposure in SORD animals) were analyzed using two-sided unpaired t-tests. Two-
177 way ANOVAs were used for analysis of interactions and main effects (genotype and diet or
178 dietary fat and dietary sucrose). Sidak's multiple comparisons test was used as post hoc analysis
179 for ANOVA tests to determine differences between groups. The difference in macronutrient
180 intake from carbohydrates was analyzed using one-way Welch's ANOVAs to correct for unequal
181 standard deviations. All tests were performed at the 95% confidence level ($\alpha = 0.05$) and groups
182 were considered significantly different when $p \leq 0.05$. No criteria were set for animal exclusion *a*
183 *priori*, and no experimental data points or animals were excluded from analysis.

184

185 **Results**

186 ***Sord* knockout does not impact erythritol synthesis in mice**

187 Loss of SORD protein was confirmed in liver and kidney by western blot (**Fig. 1A and**
188 **1B**). We found no difference in body weight or caloric intake between SORD WT and KO

189 animals on either LFD or HFD (**Fig. S1**). After 8 weeks of dietary treatment, there was a main
190 effect of *Sord* genotype on body fat percentage, however, no significant differences were
191 detected in post-hoc analysis (**Fig. S2A, genotype effect $p<0.05$**). There was also no *Sord*
192 genotype-driven difference in adipose depot weight, regardless of diet (Fig. S2B and S2C). There
193 was no significant effect of *Sord* genotype on glucose tolerance area under the curve (**Fig. S3**).

194 Fasted plasma erythritol was not modified by loss of SORD after 2 or 8 weeks of dietary
195 treatment (**Fig. 2A and 2C**). At 5 weeks, there was a significant main effect of genotype on
196 fasting plasma erythritol, but no differences were detected in specific pairwise comparisons (Fig.
197 2B, ANOVA main effect of genotype $p=0.01$). We found no effect of diet on plasma erythritol at
198 any time point (Fig. 2A-2C). There was also no effect of SORD loss on liver or kidney erythritol
199 content (**Fig 3A, 3B**). Unexpectedly, wild-type animals fed HFD had significantly less erythritol
200 in the liver and kidneys (Fig. 3A, $p<0.05$ and 3B, $p<0.01$). This effect was not observed in KO
201 mice.

202 To determine if SORD deletion results in sorbitol accumulation, we assessed plasma and
203 tissue sorbitol levels. Indeed, we found significantly elevated plasma sorbitol in KO compared to
204 WT littermates (**Fig. S4A, $p<0.0001$**). Sorbitol accumulation was further exacerbated by HFD in
205 SORD KO mice compared to LFD (Fig. S4A, $p<0.05$). Liver sorbitol was also significantly
206 elevated in SORD KO mice on LFD and HFD (Fig. S4B, $p<0.05$ and $p<0.001$ respectively).
207 There was no difference in kidney sorbitol (Fig. S4C).

208 To assess if the effect of SORD deletion on erythritol synthesis is blunted by a
209 compensatory increase in ADH1 protein levels, we quantified liver and kidney ADH1 protein.
210 We found no increase in ADH1 levels in KO compared to WT animals (**Fig. 4A and 4B**). We
211 also assessed expression of TKT, an enzyme in the non-oxidative pentose phosphate pathway

212 that has been shown to regulate erythritol synthesis in cultured cells (14). TKT expression was
213 reduced in the kidney of mice fed HFD compared to LFD (Fig. 4B, $p < 0.0001$ and $p < 0.001$ in
214 WT and KO mice, respectively), which may explain the observed reduction in kidney erythritol
215 in WT animals fed HFD (Fig 3B).

216 ***Adh1* knockout has no effect on plasma or tissue erythritol**

217 We next assessed the impact of loss of ADH1 on erythritol synthesis. ADH1 KO animals
218 displayed normal body weight, caloric intake, body composition, and glucose tolerance
219 compared to WT littermates (Fig. S5-S7). Loss of ADH1 did not impact fasting plasma erythritol
220 levels at any time point (Fig. 5). Consistent with results in SORD animals, we also found no
221 differences in plasma erythritol between diets (Fig. 5). Similarly, there was no effect of genotype
222 or diet on tissue erythritol (Fig. 6A and 6B). We did not observe any differences in SORD or
223 TKT expression in the liver or kidney between ADH1 WT and KO groups, regardless of diet
224 (Fig. 7A and 7B).

225 **Erythritol synthesis is responsive to sucrose consumption even in the absence of changes of** 226 **body weight or fasting blood glucose**

227 In SORD and ADH1 animal models, we observed no effect of HFD on circulating
228 erythritol, despite significant body weight gain and impaired glucose tolerance in HFD fed mice.
229 This suggests that erythritol synthesis in mice is not sensitive to hyperglycemia. Erythritol
230 synthesis, then, may respond to diet-induced increases in glucose availability. To test this
231 hypothesis, we provided plain drinking water or 30% sucrose solution to C57BL/6J mice fed
232 HFD for two weeks.

233 30% sucrose for two weeks did not affect body weight, although total caloric intake was
234 significantly elevated (Fig. S8A and S8B, $p < 0.01$). Fasting blood glucose was not affected by

235 30% sucrose (S8C). There was no difference in fasted plasma erythritol between groups (**Fig.**
236 **S9A**). Surprisingly, we found a 50% increase in non-fasted urine erythritol in mice fed 30%
237 sucrose in drinking water (Fig. S9B $p < 0.05$).

238 To evaluate the response of erythritol synthesis to diet more comprehensively, we utilized
239 the addition of 30% sucrose in drinking water to LFD or HFD for eight weeks. As expected,
240 mice fed HFD gained significantly more body weight over the course of 8 weeks compared to
241 LFD (**Fig. 8A**). This was consistent in both HFD with water and HFD with 30% sucrose (Fig.
242 8A, $p < 0.01$ and $p < 0.001$ respectively for effect of dietary fat). HFD also significantly increased
243 body fat percentage compared to respective LFD controls (Fig. 8B, $p < 0.0001$). There was a main
244 effect of sucrose on body fat percentage, however, no significant differences were detected in
245 pairwise comparisons (Fig. 8B, ANOVA main effect of sucrose $p < 0.05$). Sucrose water
246 significantly increased total caloric intake in mice fed LFD and HFD (Fig. 8C, $p < 0.01$). This
247 increase in total calories in mice fed sucrose water resulted from a 2-fold (LFD) and 4-fold
248 (HFD) increase in carbohydrate intake compared to plain water controls (Fig. 8D, one-way
249 ANOVA, $p < 0.0001$ and $p < 0.001$ respectively).

250 Dietary fat, but not sucrose water, contributed to changes in random and fasting blood
251 glucose (**Fig. 9A-9D**). At 5 weeks of dietary treatment mice fed HFD with 30% sucrose had
252 higher random blood glucose levels than LFD with 30% sucrose (Fig. 9B, $p < 0.05$). Fasting blood
253 glucose was significantly higher in mice fed HFD and HFD with sucrose water compared to
254 respective LFD controls (Fig. 9D, $p < 0.05$). There was no effect of sucrose water on fasting
255 glucose or random glucose at any timepoint (Fig. 9A-9D).

256 **Plasma and urine erythritol are elevated in response to sucrose water**

257 After two weeks on experimental diets, sucrose in drinking water significantly increased
258 non-fasted plasma erythritol on LFD (4.5-fold) and HFD (2.6-fold) compared to water controls
259 (**Fig. 10A, $p<0.0001$ and $p<0.05$ respectively**). Additionally, there was a significant interaction
260 between dietary fat and sucrose (Fig. 10A, ANOVA interaction $p<0.05$). Mice consuming LFD
261 with 30% sucrose had over 60% higher plasma erythritol compared to HFD with 30% sucrose
262 (Fig. 10A, $p<0.01$). The sucrose-induced increase in plasma erythritol was consistent at 2, 5 and
263 8 weeks of dietary treatment in non-fasted samples (Fig. 10A, 10B, and 10C). Following a 5-
264 hour fast, there were no differences in plasma erythritol between any of the 4 experimental diets
265 at the 7 week timepoint (Fig. 10D).

266 Urine erythritol levels paralleled plasma erythritol levels. After two weeks exposure to
267 experimental diets, there was a significant interaction between the effect of dietary fat and
268 sucrose on non-fasted urine erythritol (**Fig. 11A, ANOVA interaction $p<0.05$**). The LFD with
269 30% sucrose group was significantly higher than both LFD controls and HFD with 30% sucrose
270 (Fig. 11A, $p<0.0001$ and $p<0.01$). After 5 weeks and 8 weeks, both LFD with 30% sucrose and
271 HFD with 30% sucrose excreted significantly more erythritol than their respective controls (Fig.
272 11B and 11C). Consistent with plasma erythritol, there were no differences in fasted urine
273 erythritol content (Fig. 11D).

274 **Plasma and urine sorbitol are increased by sucrose water**

275 We also assessed plasma and urine levels of sorbitol to determine if additional
276 endogenous polyols exhibit the same response to sucrose consumption. The effect of diet on
277 plasma sorbitol levels varied across the 4 measured timepoints (**Fig S10A-S10D**). At 2 weeks,
278 there were significant main effects of fat and sucrose on plasma sorbitol, but no differences were
279 detected in pairwise comparisons (Fig. S10A, ANOVA main effect of dietary fat $p<0.05$, main

280 effect of sucrose $p < 0.05$). At 5 weeks, sucrose water significantly elevated plasma sorbitol
281 compared to water controls on LFD and HFD (Fig. S10B, $p < 0.05$). After 8 weeks, only mice fed
282 LFD with 30% sucrose had elevated plasma sorbitol compared to LFD mice (Fig. S10C,
283 $p < 0.001$). In fasted mice, plasma sorbitol was higher in HFD mice compared to LFD mice with
284 drinking water (Fig. S10D, $p < 0.05$).

285 Urine sorbitol was elevated at 2 weeks in the LFD with 30% sucrose group compared to
286 both LFD and HFD with 30% sucrose (**Fig. S11A, $p < 0.01$ and $p < 0.05$**). After 5 weeks, both
287 sucrose-fed groups had significantly higher urine sorbitol compared to water controls (Fig. S11B,
288 $p < 0.05$). There was a main effect of sucrose on urine sorbitol, but no significant pairwise
289 comparisons of urine sorbitol after 8 weeks (Fig. S11C, ANOVA main effect of sucrose $p < 0.05$).
290 There were no differences in fasting urine sorbitol (Fig. S11D).

291 **The effect of sucrose water on tissue erythritol is tissue-dependent**

292 The kidneys, liver, and quadriceps have previously been shown to synthesize erythritol
293 (13). Under low- and high-fat dietary conditions, the kidneys contain the highest levels of
294 erythritol per gram tissue, followed closely by the liver (13). We found no significant difference
295 in liver erythritol in response to sucrose water exposure (**Fig. 12A**). In the kidney, sucrose water
296 on both LFD and HFD caused a 3-fold increase in erythritol compared to respective controls
297 (Fig. 12B, $p < 0.01$). Unexpectedly, sucrose water also elevated quadriceps erythritol by more
298 than 3-fold on both LFD and 2-fold on HFD (Fig. 12C, $p < 0.001$).

299 **SORD deletion reduces tissue erythritol following exposure to sucrose water**

300 Finally, we exposed SORD WT and KO animals to LFD with 30% sucrose for two
301 weeks. We chose the SORD model based on the trend toward reduced fasted plasma erythritol on
302 LFD and HFD (Fig. 2). We expected that increasing erythritol synthesis with dietary sucrose and

303 measuring non-fasted plasma may amplify the effect of *Sord* loss. We found no difference in
304 non-fasted plasma or urine erythritol between WT and KO mice (**Fig. 13A and 13B**). In tissues,
305 there was a significant effect of genotype and tissue-type on erythritol content (Fig. 13C,
306 ANOVA main effect of genotype $p < 0.01$, main effect of tissue $p < 0.0001$). Notably, the kidneys
307 of KO animals contained 30% less erythritol than WT controls (Fig. 13C $p < 0.05$). There was no
308 difference in quadriceps erythritol between genotypes. There was also no difference in body
309 weight, food intake, or non-fasted blood glucose between genotypes (**Fig. S12A-S12C**).

310

311 **Discussion**

312 Surprisingly, we found no differences in plasma or tissue erythritol in mice lacking either
313 *Sord* or *Adh1* expression. This was true in both diet-induced obese (HFD-fed mice) and LFD-fed
314 mice (Figures 2-6), though there was a trend toward a reduction in plasma erythritol in *Sord*^{-/-}
315 mice after 5 weeks (Figure 2B). There was also no evidence of compensation for SORD or
316 ADH1 loss with an increase in protein levels of the alternative enzyme (Figures 4 and 7). This
317 suggests that basal levels of ADH1 or SORD are sufficient to maintain erythritol synthesis when
318 one is lost.

319 In cell culture models, SORD knockdown reduces erythritol synthesis only under high-
320 glucose conditions (14). We hypothesized that SORD may also only be essential for erythritol
321 synthesis when dietary sugar is in excess. To test this, we exposed SORD WT and KO mice to
322 30% sucrose in drinking water for two weeks, a relatively short exposure that did not result in
323 effects on body weight (Fig S12A). There was no effect of *Sord* genotype on plasma or urine
324 erythritol in response to sugar overfeeding (Figure 12). There was, however, a 30% reduction in
325 kidney erythritol in SORD KO mice after sugar overfeeding.

326 Our findings also indicate that neither excess caloric intake from fat nor hyperglycemia
327 are the driving factor in erythritol synthesis in young mice. Mice fed HFD exhibited elevated
328 caloric intake, body weight gain, and fasting glucose compared to LFD controls with no
329 significant difference in erythritol synthesis (Figures 8 and 10). In contrast, exposure to 30%
330 sucrose in drinking water elevated non-fasted plasma and urine erythritol over the course of 8
331 weeks (Figures 10 and 11). Mice fed LFD with 30% sucrose water consistently exhibited the
332 highest plasma and urine erythritol content (Figures 10 and 11). These mice consumed more
333 calories from sugar than any other dietary treatment (Figure 8D). Mice fed HFD with 30% sugar
334 water also exhibited elevated non-fasting plasma and urine erythritol compared to water controls,
335 but lower plasma and urine erythritol levels than mice consuming LFD with 30% sucrose
336 (Figures 10 and 11). The difference between these sucrose-exposure groups is likely due to the
337 amount of sugar water consumed in the LFD group, rather than an interaction between dietary fat
338 and dietary sugar. On average, mice fed LFD with 30% sucrose consumed 55% more calories
339 from sugar water than mice fed HFD with 30% sucrose (Fig 8D).

340 Erythritol synthesis *in vivo* appears to be controlled by simple sugar consumption rather
341 than total carbohydrate intake. This is supported by the comparison of plasma and urinary
342 erythritol in LFD and HFD-fed mice. The LFD (10% FDC) contains more carbohydrates than the
343 HFD (60% FDC). However, there is no difference in circulating erythritol levels between mice
344 exposed to these diets (Figure 10). The primary carbohydrate source in the 10% FDC diet is
345 cornstarch, which makes up 40% of the calories. Cornstarch is primarily composed of
346 amylopectin, a branching, slowly digested chain of glucose that has a low glycemic index
347 (18,19). Erythritol synthesis appears to respond to rapid (i.e. sucrose in drinking water) rather
348 than slowly digestible carbohydrates. Other studies have shown differences between liquid and

349 solid sucrose administration on the metabolic response to sugar in mice (20,21). Further studies
350 are required to determine if erythritol synthesis is consistently elevated by simple, not complex
351 carbohydrate intake when controlling for mode of administration (liquid/solid).

352 In humans, elevated erythritol in fasting plasma is a biomarker for cardiometabolic
353 disease risk (1–3). Despite significant elevation in non-fasted circulating erythritol, we found no
354 impact of diet on fasted plasma or urine erythritol levels (Figures 10C and 11C). There are
355 several factors that may contribute to the lack of changes in fasting plasma erythritol in mouse
356 models. This work was performed in young, healthy mice, whereas the human observational
357 studies have largely been performed on middle-aged participants (2,3,5–8,10). These findings
358 may also reflect species-specific differences in metabolism. Mice have an overall more rapid
359 metabolism and higher glucose turnover compared to humans (22,23). In addition, fasting mice
360 deplete available glucose more rapidly than humans and are more reliant on gluconeogenesis to
361 maintain glucose homeostasis (22,23). The rapid depletion of glucose stores in fasting mice may
362 limit the production of erythritol from glucose catabolism. To overcome the limitation of mouse
363 models, future work in humans is required to determine if sugar consumption contributes to
364 elevated fasting erythritol.

365 Finally, we found that sucrose water elevated kidney and quadriceps erythritol content,
366 while liver erythritol content was stable across all diets (Figure 12). Differences in liver
367 erythritol may have been dampened by lipid accumulation on sucrose diets. During tissue
368 erythritol quantification, polar metabolites are normalized to tissue wet weight, which is elevated
369 by lipid deposition and may reduce the relative erythritol content per gram of tissue. Overall,
370 however, it appears that the liver is not driving sucrose-induced erythritol synthesis. Elevated
371 kidney erythritol was an expected response based on previous work in human proximal tubule

372 cells in which high glucose media increased intracellular erythritol (14,24). Elevated circulating
373 erythritol is also associated with markers of impaired kidney function (11,25).

374 This is the first report of elevated erythritol in skeletal muscle in response to glucose
375 availability (Figure 12C). This was unexpected based on the low expression and activity of
376 pentose phosphate pathway enzymes in skeletal muscle and the relatively low quadriceps
377 erythritol content compared to liver and kidneys (13,26,27). In humans, however, Lustgarten and
378 Fielding recently observed a negative association between skeletal muscle density and serum
379 erythritol levels (25). Pentose phosphate pathway enzymes have also been shown to increase in
380 mouse skeletal muscle in response to high-fat diet exposure, and muscle glucose-6-phosphate
381 dehydrogenase (G6PD) expression is associated with impaired glucose metabolism (26,28,29).
382 Historically, increased PPP activity has been reported following skeletal muscle injury and in
383 disordered skeletal muscle (30,31). Taken together, these findings suggest that circulating
384 erythritol may be indicative of impaired skeletal muscle metabolism.

385 The skeletal muscle may also be a useful model for further understanding the regulation
386 of erythritol synthesis. Although quadriceps appear to have lower erythritol content compared to
387 the liver and kidneys, this represents a small percentage of total body skeletal muscle (13).
388 Skeletal muscle is responsible for around 30% of postprandial glucose disposal (whereas the
389 kidney disposes of only 7%) and may therefore contribute more to circulating erythritol levels
390 than is captured by a single tissue sample (22). It is notable that the erythritol-synthesizing
391 enzymes ADH1 and SORD were originally identified and purified from rabbit liver (12). Muscle
392 ADH1 and SORD protein levels are relatively low, which makes it an ideal tissue to identify
393 alternative enzymes that catalyze the conversion of erythrose to erythritol (32). The modest

394 expression of ADH1 and SORD in skeletal muscle may also have blunted the effect of
395 *Adh1/Sord* knockout on plasma erythritol levels.

396 A limitation of this study is that protein intake was not constant between the 30% sucrose
397 and the water control groups. *Ad libidum* access to sucrose solution reduced solid food intake in
398 both LFD with 30% sucrose and HFD with 30% sucrose mice, resulting in a decrease in protein
399 intake. Future studies may be able to account for protein intake with pair feeding, which is
400 beyond the scope of this work. Circulating erythritol was proportional to the amount of sucrose
401 water consumed, suggesting that sucrose was the primary determinant of elevated erythritol
402 levels in the present study.

403 In conclusion, we found that sucrose intake significantly elevated erythritol synthesis and
404 excretion in mice. Erythritol synthesis and excretion is a novel pathway for the disposal of
405 glucose carbons when dietary sugar is in excess. Future studies in humans should assess if there
406 is an association between simple sugar intake and erythritol in plasma and/or skeletal muscle.

407

408 **Acknowledgements**

409 The authors thank Peyton Carpen and Brian Walker for assistance with data collection and the
410 Cornell Statistical Consulting Unit for assistance with data analysis.

411

412 **Author Contributions**

413 SRO and MSF designed research; SRO conducted research and analyzed data; SRO and MSF
414 wrote the paper. MSF had primary responsibility for final content. All authors have read and
415 approved the final manuscript.

416

417 **References**

- 418 1. Ortiz SR, Field MS. Mammalian metabolism of erythritol: a predictive biomarker of
419 metabolic dysfunction. *Curr Opin Clin Nutr Metab Care* 2020;23:296–301.
- 420 2. Rebholz CM, Yu B, Zheng Z, Chang P, Tin A, Köttgen A, Wagenknecht LE, Coresh J,
421 Boerwinkle E, Selvin E. Serum metabolomic profile of incident diabetes. *Diabetologia*
422 [Internet] 2018;61:1046–54. Available from:
423 <https://www.ncbi.nlm.nih.gov/pmc/articles/PMC5878141/>
- 424 3. Wang Z, Zhu C, Nambi V, Morrison AC, Folsom AR, Ballantyne CM, Boerwinkle E, Yu
425 B. Metabolomic Pattern Predicts Incident Coronary Heart Disease: Findings From the
426 Atherosclerosis Risk in Communities Study. *Arterioscler Thromb Vasc Biol* [Internet] 2019
427 [cited 2019 Nov 12];39:1475–82. Available from:
428 <https://www.ahajournals.org/doi/10.1161/ATVBAHA.118.312236>
- 429 4. Hootman KC, Trezzi J-P, Kraemer L, Burwell LS, Dong X, Guertin KA, Jaeger C, Stover
430 PJ, Hiller K, Cassano PA. Erythritol is a pentose-phosphate pathway metabolite and
431 associated with adiposity gain in young adults. *Proc Natl Acad Sci* [Internet] 2017 [cited
432 2018 Oct 29];114:E4233–40. Available from:
433 <http://www.pnas.org/lookup/doi/10.1073/pnas.1620079114>
- 434 5. Murthy VL, Yu B, Wang W, Zhang X, Alkis T, Pico AR, Yeri A, Bhupathiraju SN,
435 Bressler J, Ballantyne CM, et al. Molecular Signature of Multisystem Cardiometabolic
436 Stress and Its Association With Prognosis. *JAMA Cardiol* [Internet] 2020 [cited 2020 Jul
437 29]; Available from: <https://jamanetwork.com/journals/jamacardiology/fullarticle/2768738>
- 438 6. Suhre K, Meisinger C, Döring A, Altmaier E, Belcredi P, Gieger C, Chang D, Milburn MV,
439 Gall WE, Weinberger KM, et al. Metabolic Footprint of Diabetes: A Multiplatform
440 Metabolomics Study in an Epidemiological Setting. *PLoS ONE* [Internet] 2010;5.
441 Available from: <https://www.ncbi.nlm.nih.gov/pmc/articles/PMC2978704/>
- 442 7. Menni C, Fauman E, Erte I, Perry JRB, Kastenmüller G, Shin S-Y, Petersen A-K, Hyde C,
443 Psatha M, Ward KJ, et al. Biomarkers for Type 2 Diabetes and Impaired Fasting Glucose
444 Using a Nontargeted Metabolomics Approach. *Diabetes* [Internet] 2013;62:4270–6.
445 Available from: <https://www.ncbi.nlm.nih.gov/pmc/articles/PMC3837024/>
- 446 8. Deidda M, Noto A, Cadeddu Dessalvi C, Andreini D, Andreotti F, Ferrannini E, Latini R,
447 Maggioni AP, Magnoni M, Mercurio G, et al. Why Do High-Risk Patients Develop or Not
448 Develop Coronary Artery Disease? Metabolic Insights from the CAPIRE Study.
449 *Metabolites* [Internet] 2022 [cited 2022 Feb 27];12:123. Available from:
450 <https://www.mdpi.com/2218-1989/12/2/123>
- 451 9. Jain R, Özgümüş T, Jensen TM, du Plessis E, Keindl M, Møller CL, Falhammar H,
452 Nyström T, Catrina S-B, Jörneskog G, et al. Liver nucleotide biosynthesis is linked to
453 protection from vascular complications in individuals with long-term type 1 diabetes. *Sci*

- 454 Rep [Internet] 2020 [cited 2020 Dec 12];10. Available from:
455 <http://www.nature.com/articles/s41598-020-68130-y>
- 456 10. Katakami N, Omori K, Taya N, Arakawa S, Takahara M, Matsuoka T, Tsugawa H, Furuno
457 M, Bamba T, Fukusaki E, et al. Plasma metabolites associated with arterial stiffness in
458 patients with type 2 diabetes. *Cardiovasc Diabetol* [Internet] 2020 [cited 2020 Dec 12];19.
459 Available from: <https://cardiab.biomedcentral.com/articles/10.1186/s12933-020-01057-w>
- 460 11. Haukka JK, Sandholm N, Forsblom C, Cobb JE, Groop P-H, Ferrannini E. Metabolomic
461 Profile Predicts Development of Microalbuminuria in Individuals with Type 1 Diabetes. *Sci*
462 *Rep* 2018;8:13853.
- 463 12. Schlicker L, Szebenyi DME, Ortiz SR, Heinz A, Hiller K, Field MS. Unexpected roles for
464 ADH1 and SORD in catalyzing the final step of erythritol biosynthesis. *J Biol Chem*
465 [Internet] 2019 [cited 2019 Oct 23];jbc.RA119.009049. Available from:
466 <http://www.jbc.org/content/early/2019/09/11/jbc.RA119.009049>
- 467 13. Ortiz SR, Field MS. Chronic Dietary Erythritol Exposure Elevates Plasma Erythritol
468 Concentration in Mice but Does Not Cause Weight Gain or Modify Glucose Homeostasis. *J*
469 *Nutr* [Internet] 2021 [cited 2021 Sep 28];151:2114–24. Available from:
470 <https://academic.oup.com/jn/article/151/8/2114/6294069>
- 471 14. Ortiz SR, Heinz A, Hiller K, Field MS. Erythritol synthesis is elevated in response to
472 oxidative stress and regulated by the non-oxidative pentose phosphate pathway in A549
473 cells. *Front Nutr* [Internet] 2022 [cited 2022 Oct 31];9:953056. Available from:
474 <https://www.frontiersin.org/articles/10.3389/fnut.2022.953056/full>
- 475 15. Deltour L, Foglio MH, Duester G. Metabolic deficiencies in alcohol dehydrogenase Adh1,
476 Adh3, and Adh4 null mutant mice. Overlapping roles of Adh1 and Adh4 in ethanol
477 clearance and metabolism of retinol to retinoic acid. *J Biol Chem* 1999;274:16796–801.
- 478 16. Chew JL, Chua KY. Collection of Mouse Urine for Bioassays. *Lab Anim* [Internet] 2003
479 [cited 2022 Jun 20];32:48–50. Available from: [http://www.nature.com/articles/labn0803-](http://www.nature.com/articles/labn0803-48)
480 48
- 481 17. Bensadoun A, Weinstein D. Assay of proteins in the presence of interfering materials. *Anal*
482 *Biochem* 1976;70:241–50.
- 483 18. Hamaker BR, Tuncil YE, Shen X. Chapter 11 - Carbohydrates of the Kernel. In: Serna-
484 Saldivar SO, editor. *Corn* (Third Edition). [Internet] Oxford: AACC International Press;
485 2019 [cited 2022 Jul 21]. p. 305–18. Available from:
486 <https://www.sciencedirect.com/science/article/pii/B9780128119716000115>
- 487 19. Cummings JH, Englyst HN. Gastrointestinal effects of food carbohydrate. *Am J Clin Nutr*
488 [Internet] 1995 [cited 2022 Jul 21];61:938S-945S. Available from:
489 <https://doi.org/10.1093/ajcn/61.4.938S>

- 490 20. Togo J, Hu S, Li M, Niu C, Speakman JR. Impact of dietary sucrose on adiposity and
491 glucose homeostasis in C57BL/6J mice depends on mode of ingestion: liquid or solid. *Mol*
492 *Metab* [Internet] 2019 [cited 2022 Jul 21];27:22–32. Available from:
493 <https://www.ncbi.nlm.nih.gov/pmc/articles/PMC6717800/>
- 494 21. Ritze Y, Bárdos G, D’Haese JG, Ernst B, Thurnheer M, Schultes B, Bischoff SC. Effect of
495 High Sugar Intake on Glucose Transporter and Weight Regulating Hormones in Mice and
496 Humans. *PLOS ONE* [Internet] Public Library of Science; 2014 [cited 2022 Jul
497 21];9:e101702. Available from:
498 <https://journals.plos.org/plosone/article?id=10.1371/journal.pone.0101702>
- 499 22. Kowalski GM, Bruce CR. The regulation of glucose metabolism: implications and
500 considerations for the assessment of glucose homeostasis in rodents. *Am J Physiol-*
501 *Endocrinol Metab* [Internet] 2014 [cited 2022 Jul 21];307:E859–71. Available from:
502 <https://www.physiology.org/doi/10.1152/ajpendo.00165.2014>
- 503 23. Fuller KNZ, Thyfault JP. Barriers in translating preclinical rodent exercise metabolism
504 findings to human health. *J Appl Physiol* [Internet] 2021 [cited 2022 Jul 21];130:182–92.
505 Available from: <https://journals.physiology.org/doi/10.1152/jappphysiol.00683.2020>
- 506 24. Valdés A, Lucio-Cazaña FJ, Castro-Puyana M, García-Pastor C, Fiehn O, Marina ML.
507 Comprehensive metabolomic study of the response of HK-2 cells to hyperglycemic hypoxic
508 diabetic-like milieu. *Sci Rep* [Internet] 2021 [cited 2021 Dec 11];11:5058. Available from:
509 <http://www.nature.com/articles/s41598-021-84590-2>
- 510 25. Lustgarten MS, Fielding RA. Metabolites related to renal function, immune activation, and
511 carbamylation are associated with muscle composition in older adults. *Exp Gerontol*
512 [Internet] 2017 [cited 2022 Jul 21];100:1–10. Available from:
513 <https://www.sciencedirect.com/science/article/pii/S0531556517304734>
- 514 26. Jiang A, Guo H, Jiang X, Tao J, Wu W, Liu H. G6PD Deficiency Is Crucial for Insulin
515 Signaling Activation in Skeletal Muscle. *Int J Mol Sci* [Internet] Multidisciplinary Digital
516 Publishing Institute; 2022 [cited 2022 Jul 21];23:7425. Available from:
517 <https://www.mdpi.com/1422-0067/23/13/7425>
- 518 27. Cabezas H, Raposo RR, Meléndez-Hevia E. Activity and metabolic roles of the pentose
519 phosphate cycle in several rat tissues. *Mol Cell Biochem* 1999;201:57–63.
- 520 28. Liu Y, Turdi S, Park T, Morris NJ, Deshaies Y, Xu A, Sweeney G. Adiponectin Corrects
521 High-Fat Diet–Induced Disturbances in Muscle Metabolomic Profile and Whole-Body
522 Glucose Homeostasis. *Diabetes* [Internet] 2013 [cited 2022 Jul 21];62:743–52. Available
523 from: <https://doi.org/10.2337/db12-0687>
- 524 29. Lund J, Ouwens DM, Wettergreen M, Bakke SS, Thoresen GH, Aas V. Increased
525 Glycolysis and Higher Lactate Production in Hyperglycemic Myotubes. *Cells* [Internet]
526 Multidisciplinary Digital Publishing Institute; 2019 [cited 2022 Jul 21];8:1101. Available
527 from: <https://www.mdpi.com/2073-4409/8/9/1101>

- 528 30. Wagner KR, Kauffman FC, Max SR. The pentose phosphate pathway in regenerating
529 skeletal muscle. *Biochem J* [Internet] 1978 [cited 2022 Jul 21];170:17–22. Available from:
530 <https://europepmc.org/articles/PMC1183856>
- 531 31. Meijer AE. The pentose phosphate pathway in skeletal muscle under patho-physiological
532 conditions. A combined histochemical and biochemical study. *Prog Histochem Cytochem*
533 1991;22:1–118.
- 534 32. Uhlén M, Fagerberg L, Hallström BM, Lindskog C, Oksvold P, Mardinoglu A, Sivertsson
535 Å, Kampf C, Sjöstedt E, Asplund A, et al. Tissue-based map of the human proteome.
536 *Science* [Internet] American Association for the Advancement of Science; 2015 [cited 2022
537 Jul 21];347:1260419. Available from:
538 <https://www.science.org/doi/10.1126/science.1260419>

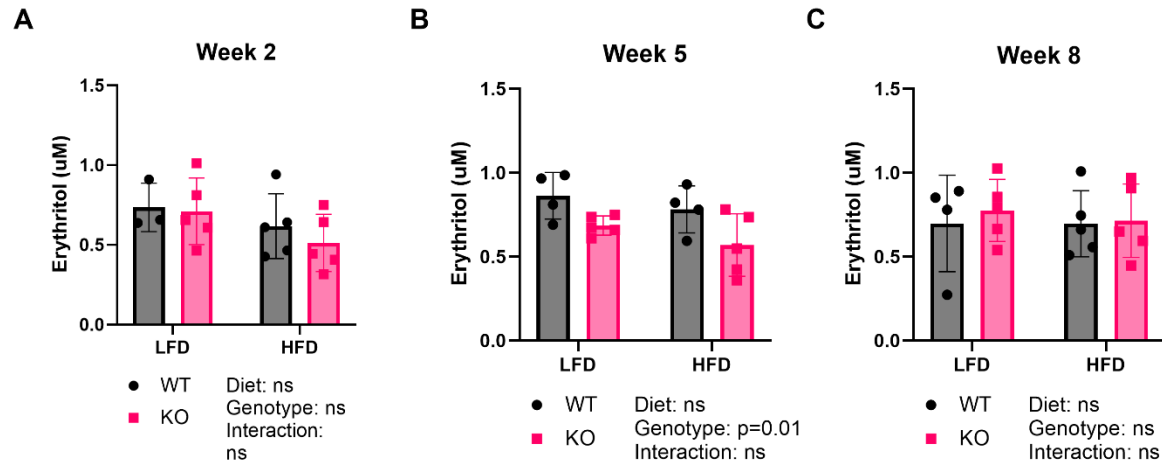
539

540 **Figures**



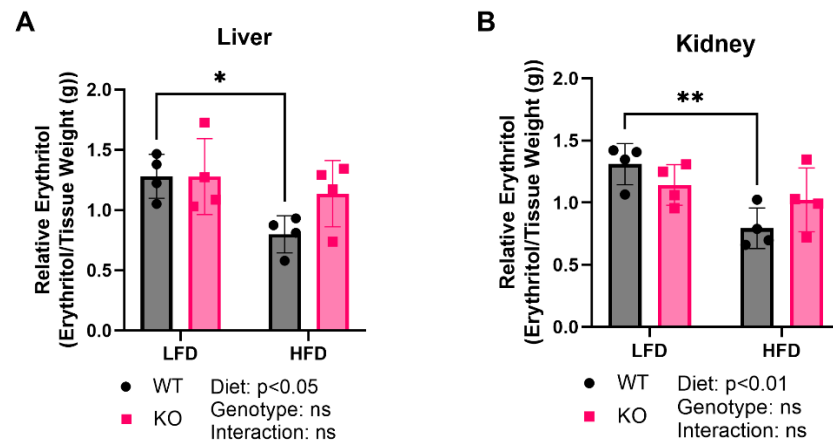
541

542 **Figure 1. Single base deletion in exon 4 eliminates liver and kidney SORD protein.** SORD
543 protein is absent in A) liver and B) kidney of 8-week-old KO mice. Data points represent tissues
544 harvested from individual mice (n=3). ATUB: alpha tubulin; KO: knockout; SORD: sorbitol
545 dehydrogenase; WT: wildtype.



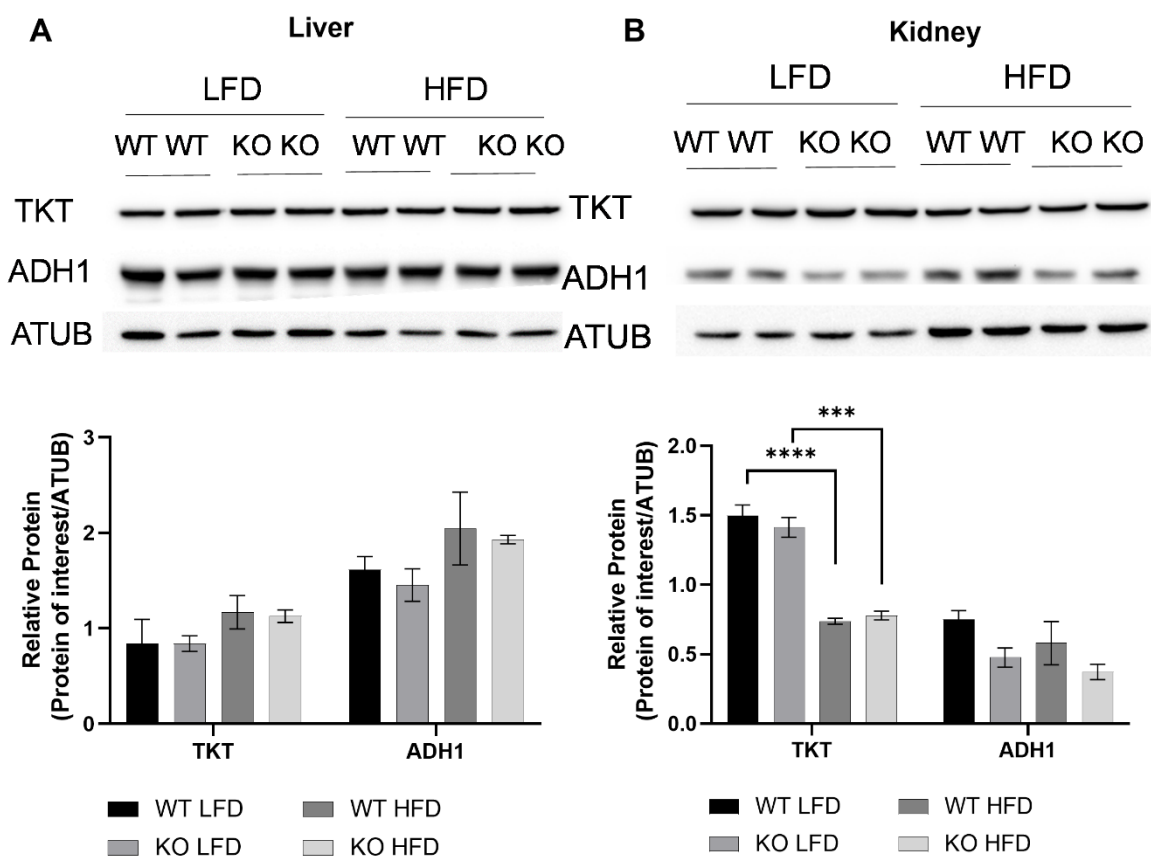
546

547 **Figure 2. Loss of SORD does not affect plasma erythritol in mice fed LFD or HFD.** Plasma
548 erythritol in SORD WT and KO mice following A) 2 weeks, B) 5 weeks, and C) 8 weeks of
549 treatment with LFD or HFD. Data presented as mean \pm SD. HFD: high-fat diet; KO: knockout;
550 LFD: low-fat diet; WT: wildtype.



551

552 **Figure 3. Loss of SORD does not affect tissue erythritol in mice fed LFD or HFD.** Relative
553 erythritol content of A) liver and B) kidney of SORD WT and KO mice after 8 weeks on
554 experimental diets. Data presented as mean \pm SD. *p<0.05, **p<0.01. HFD: high-fat diet; KO:
555 knockout; LFD: low-fat diet; WT: wildtype.



556

557 **Figure 4. *Sord* genotype does not impact TKT or ADH1 levels in liver and kidney.**

558 Representative western blot and densitometry quantification of enzymes TKT and ADH1 in A)

559 liver and B) kidney of *SORD* WT and KO mice after 8 weeks of dietary treatment. Data points

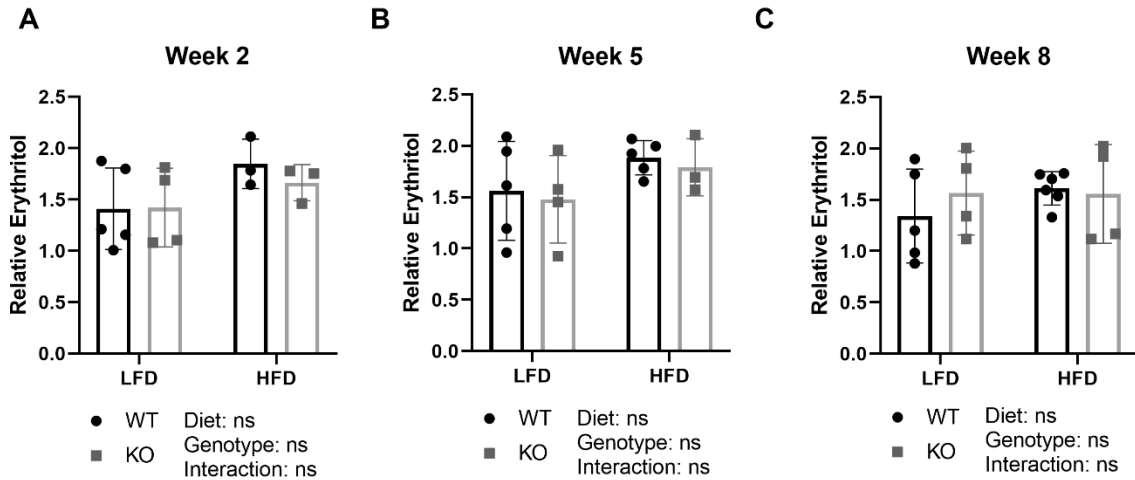
560 represent tissue harvested from individual mice (n=2) and quantification is presented as mean ±

561 SD. Differences between groups are analyzed by two-way ANOVA. *p<0.05, **p<0.01,

562 ***p<0.001, ****p<0.0001. ADH1: alcohol dehydrogenase 1; ATUB: alpha tubulin; HFD: high-

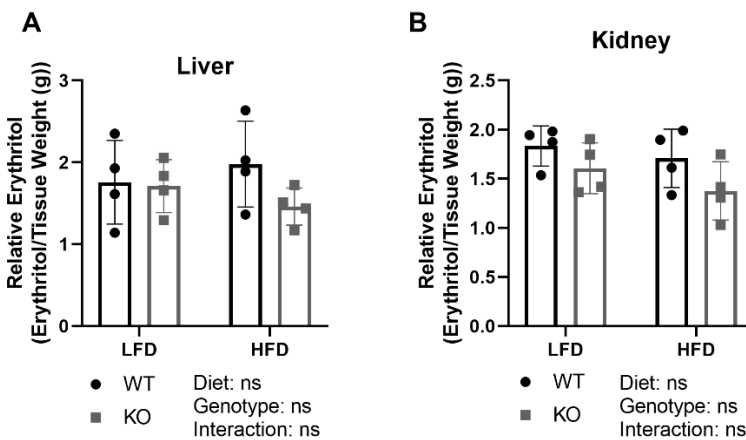
563 fat diet; KO: knockout; LFD: low-fat diet; *SORD*: sorbitol dehydrogenase; TKT: transketolase;

564 WT: wildtype.



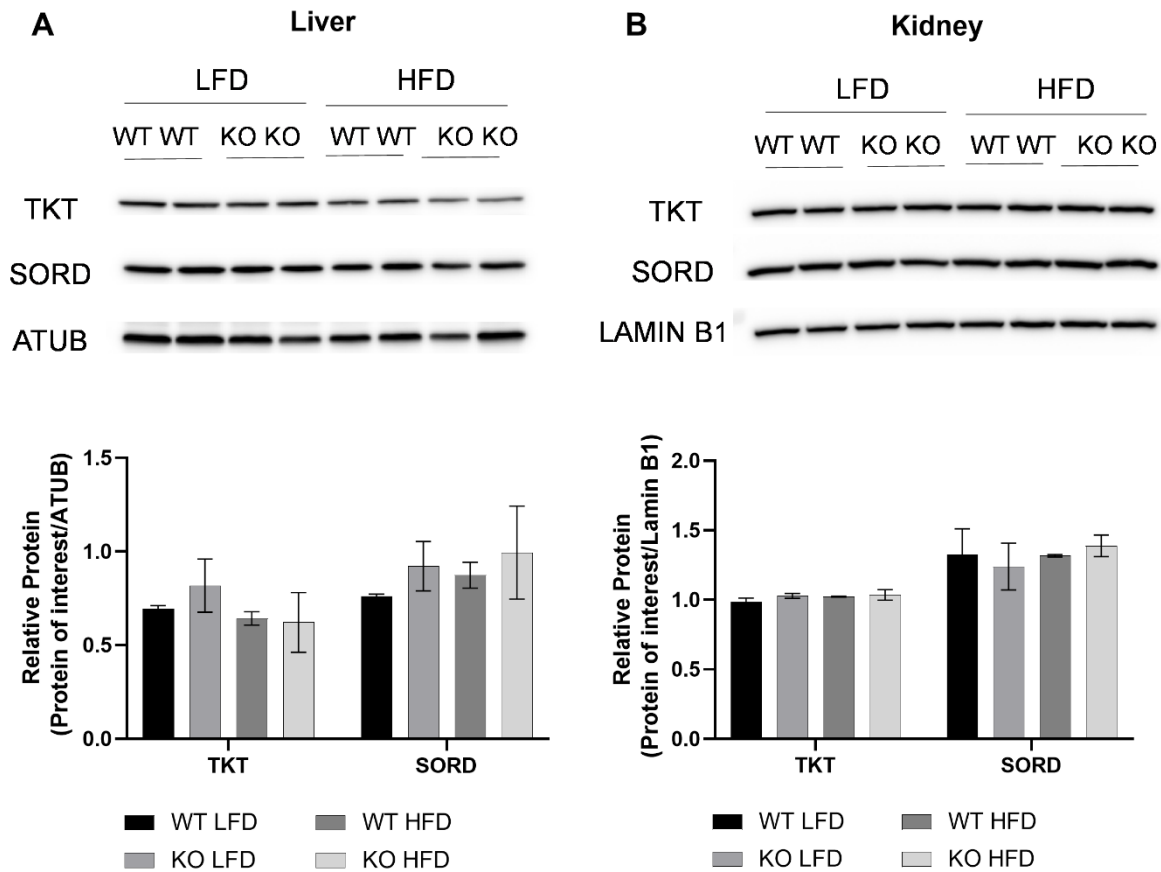
565

566 **Figure 5. Plasma erythritol is not impacted by *Adh1* knockout.** Plasma erythritol in ADH1
567 WT and KO mice following A) 2 weeks, B) 5 weeks, and C) 8 weeks of treatment with LFD or
568 HFD. Data presented as mean \pm SD. HFD: high-fat diet; KO: knockout; LFD: low-fat diet; WT:
569 wildtype.



570

571 **Figure 6. *Adh1* deletion does not significantly decrease liver or kidney erythritol.** Relative
572 erythritol content of A) liver and B) kidney of ADH1 WT and KO mice after 8 weeks on
573 experimental diets. Data presented as mean \pm SD. HFD: high-fat diet; KO: knockout; LFD: low-
574 fat diet; WT: wildtype.



575

576 **Figure 7. *Adh1* genotype does not impact TKT or SORD expression in liver and kidney.**

577 Representative western blot and densitometry quantification of enzymes TKT and SORD in A)

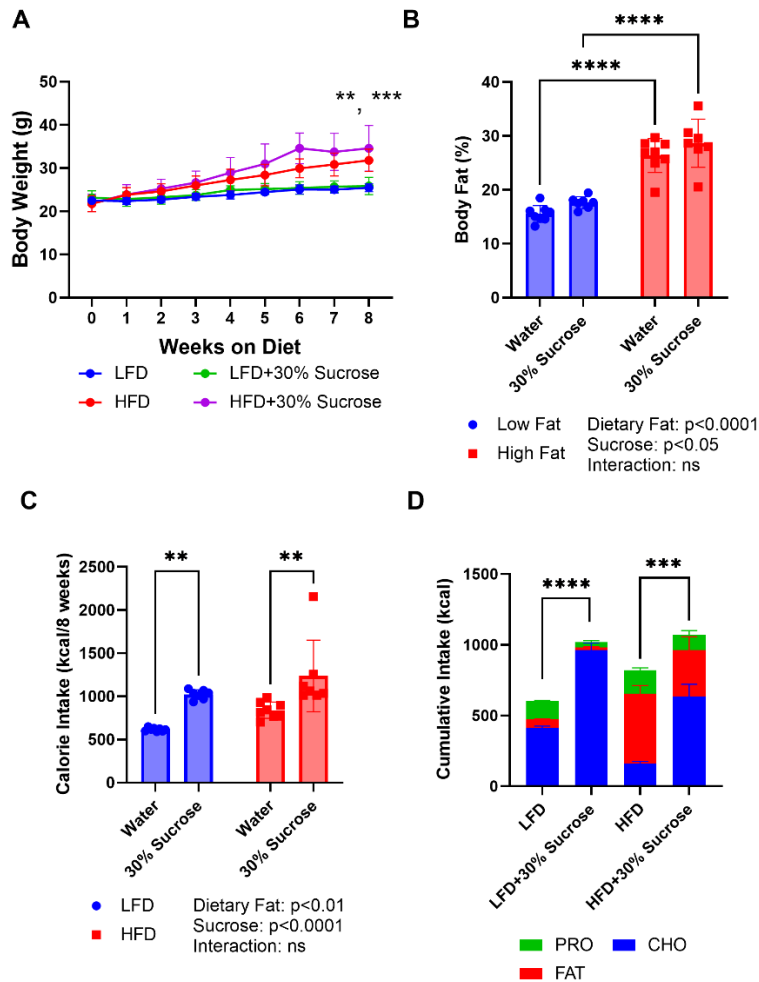
578 liver and B) kidney of ADH1 WT and KO mice after 8 weeks of dietary treatment. Data points

579 represent tissue harvested from individual mice (n=2) and quantification is presented as mean \pm

580 SD. Differences between groups are analyzed by two-way ANOVA. ADH1: alcohol

581 dehydrogenase 1; ATUB: alpha tubulin; HFD: high-fat diet; KO: knockout; LFD: low-fat diet;

582 SORD: sorbitol dehydrogenase; TKT: transketolase; WT: wildtype.



583

584 **Figure 8. Sucrose in drinking water significantly increased caloric intake, body weight and**

585 **fat percentage.** A) Weekly body weight in grams, asterisks indicate p-value comparing LFD to

586 HFD and LFD + 30% sucrose to HFD + 30% sucrose, respectively, at the 8-week timepoint. B)

587 Body fat percentage following 8 weeks of dietary treatment measured by NMR. C) Total

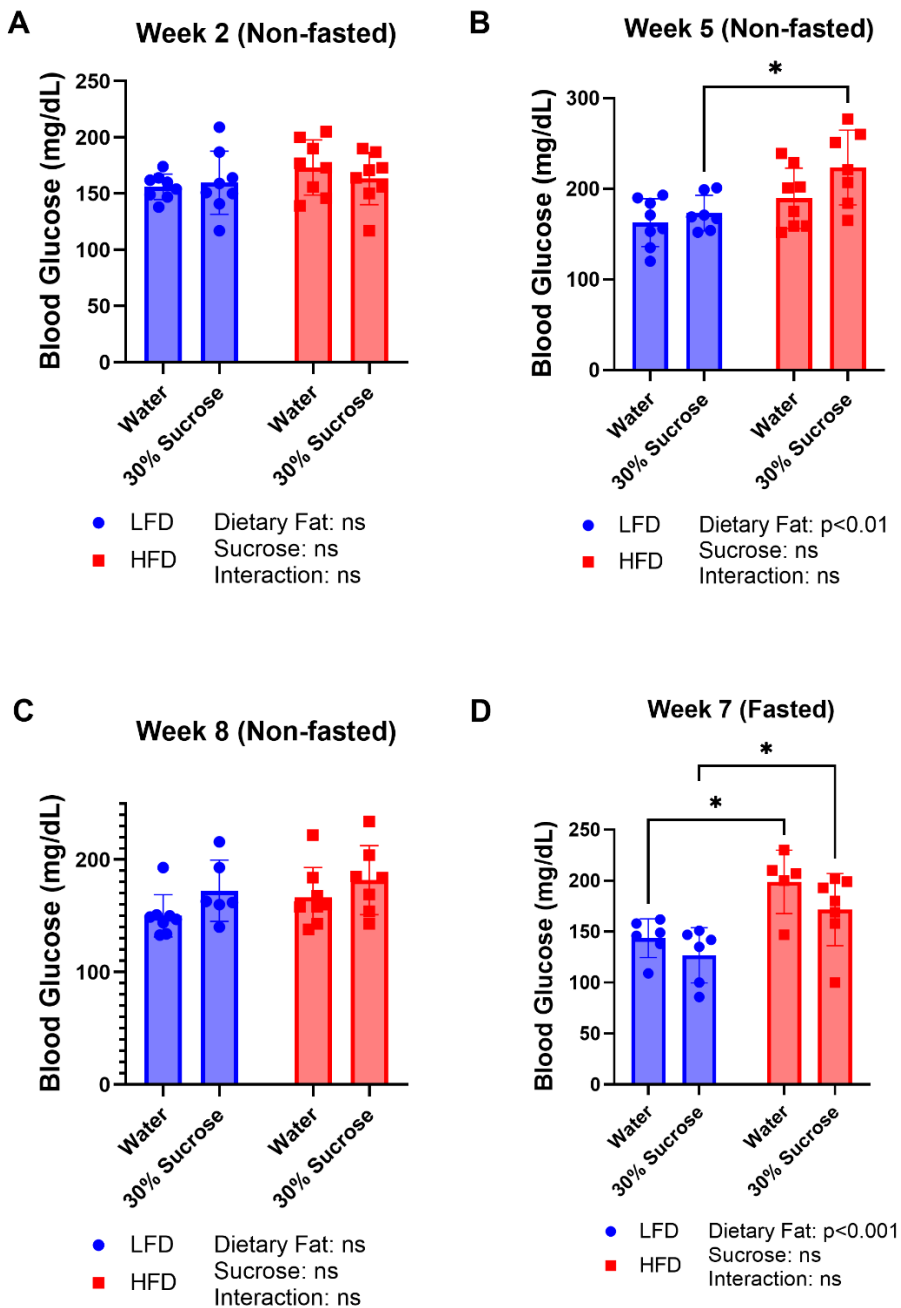
588 cumulative caloric intake in kilocalories (kcal). D) Proportion of total caloric intake from

589 protein, carbohydrates, and fat in each experimental diet. Asterisks represent results of a one-way

590 Welch's ANOVA comparing cumulative intake from carbohydrates. Data are expressed as mean

591 \pm SD. ** $p < 0.01$, *** $p < 0.001$, **** $p < 0.0001$. CHO: carbohydrate; HFD: high-fat diet; LFD:

592 low-fat diet; PRO: protein.



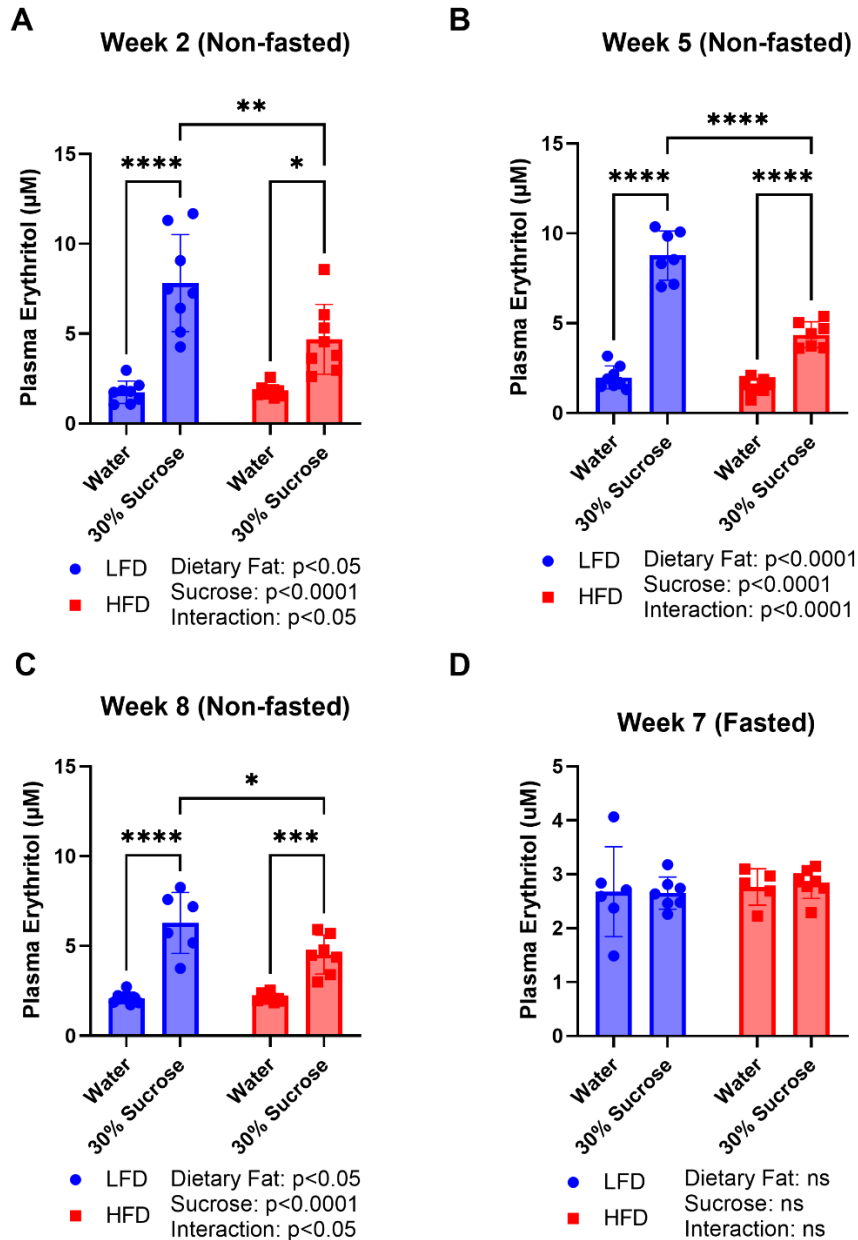
593

594 **Figure 9. Sucrose in drinking water did not significantly impact fed or fasted blood glucose.**

595 Blood glucose in non-fasted mice at A) 2 weeks, B) 5 weeks, and C) 8 weeks of diet treatment.

596 D) Blood glucose in fasted mice after 7 weeks of dietary treatment. Data are presented as mean \pm

597 SD. *p<0.05. HFD: high-fat diet; LFD: low-fat diet.



598

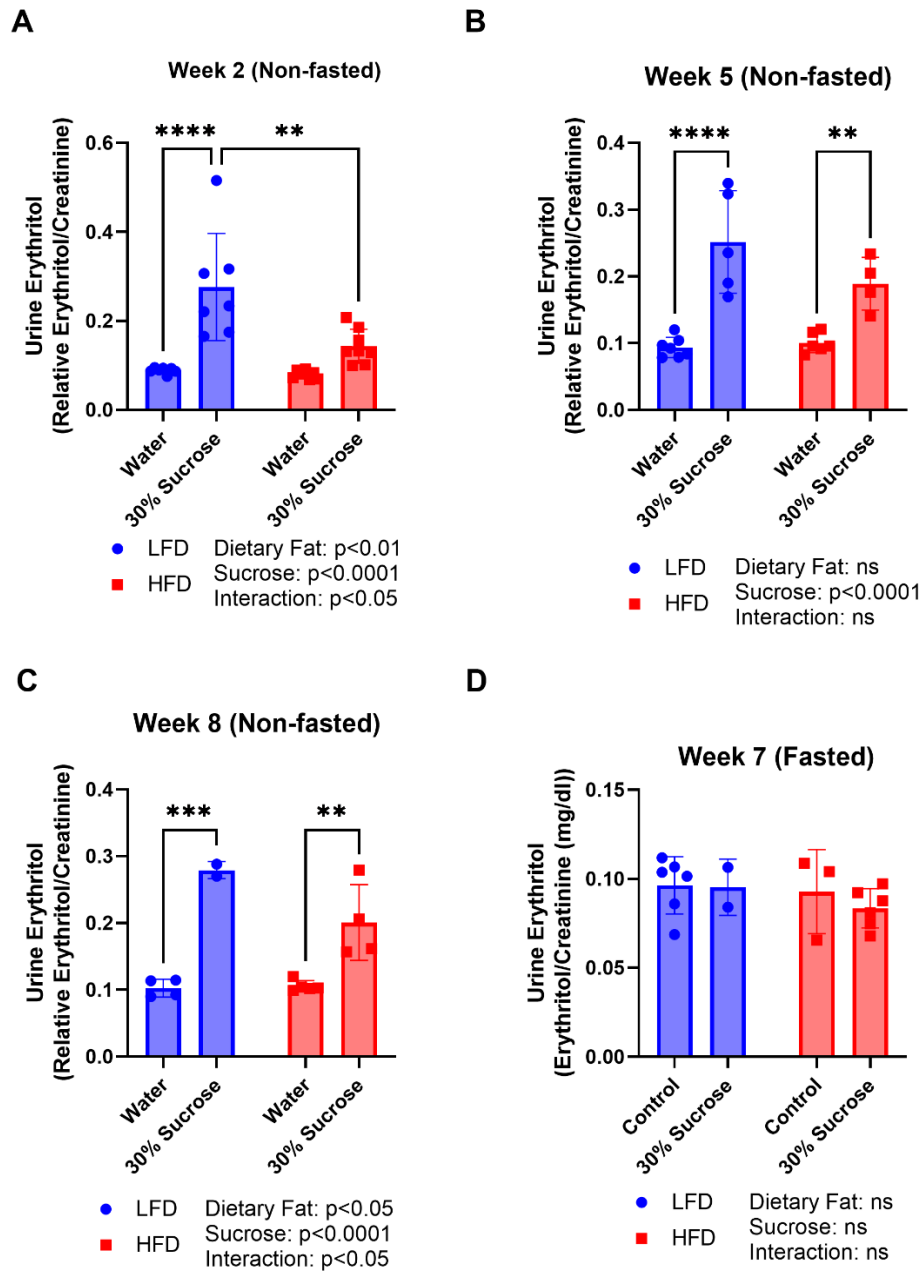
599 **Figure 10. Plasma erythritol is significantly elevated by sucrose in fed, but not fasted mice.**

600 Plasma erythritol in non-fasted mice at A) 2 weeks, B) 5 weeks, and C) 8 weeks of diet

601 treatment. D) Plasma erythritol in fasted mice after 7 weeks of dietary treatment. Data are

602 presented as mean \pm SD. * $p < 0.05$, ** $p < 0.01$, *** $p < 0.001$, **** $p < 0.0001$. HFD: high-fat diet;

603 LFD: low-fat diet.



604

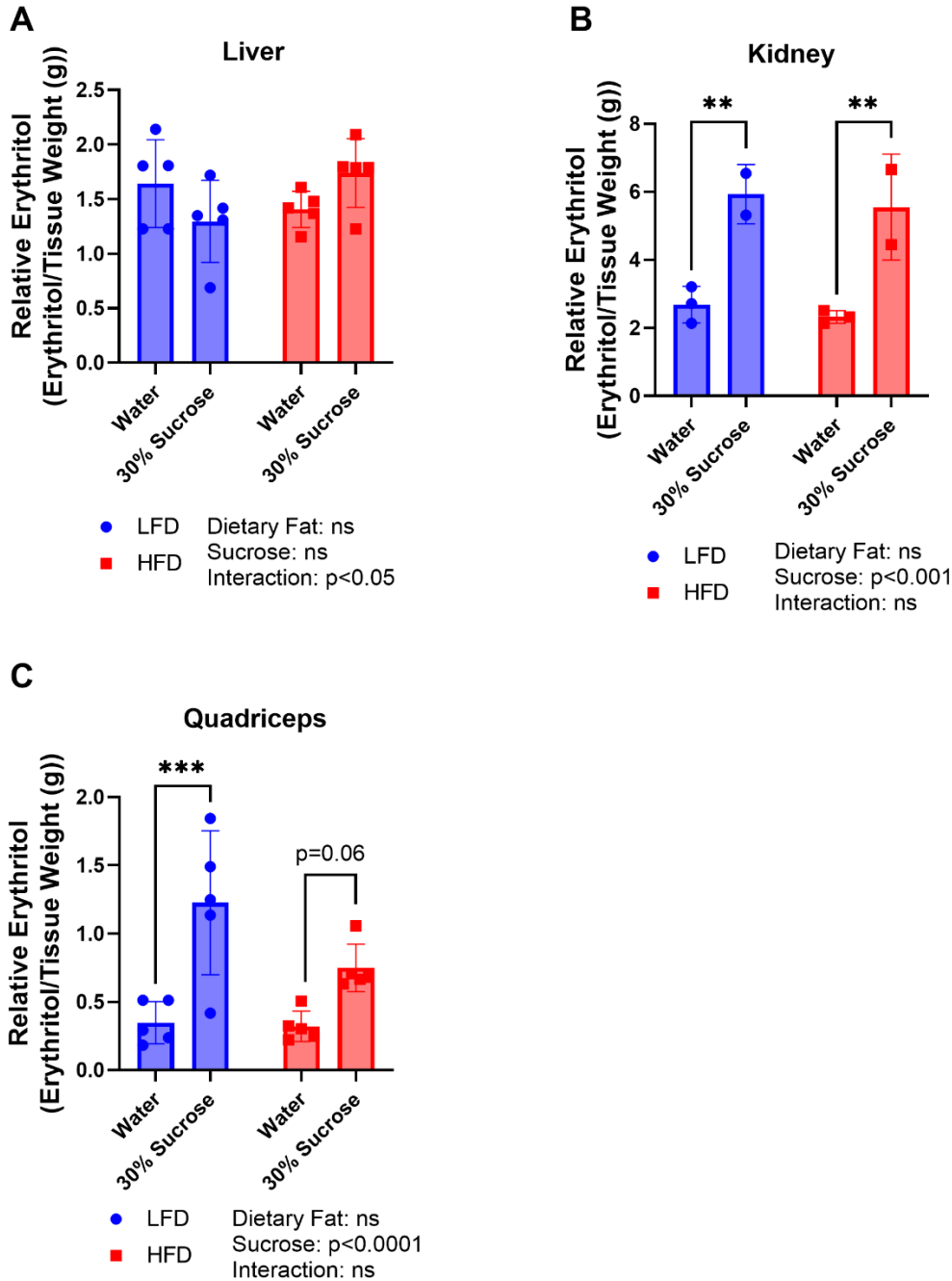
605 **Figure 11. Urinary erythritol is elevated by sucrose in drinking water in fed mice.** Relative

606 urinary erythritol in non-fasted mice at A) 2 weeks, B) 5 weeks, and C) 8 weeks of diet

607 treatment. D) Relative urinary erythritol in fasted mice after 7 weeks of dietary treatment.

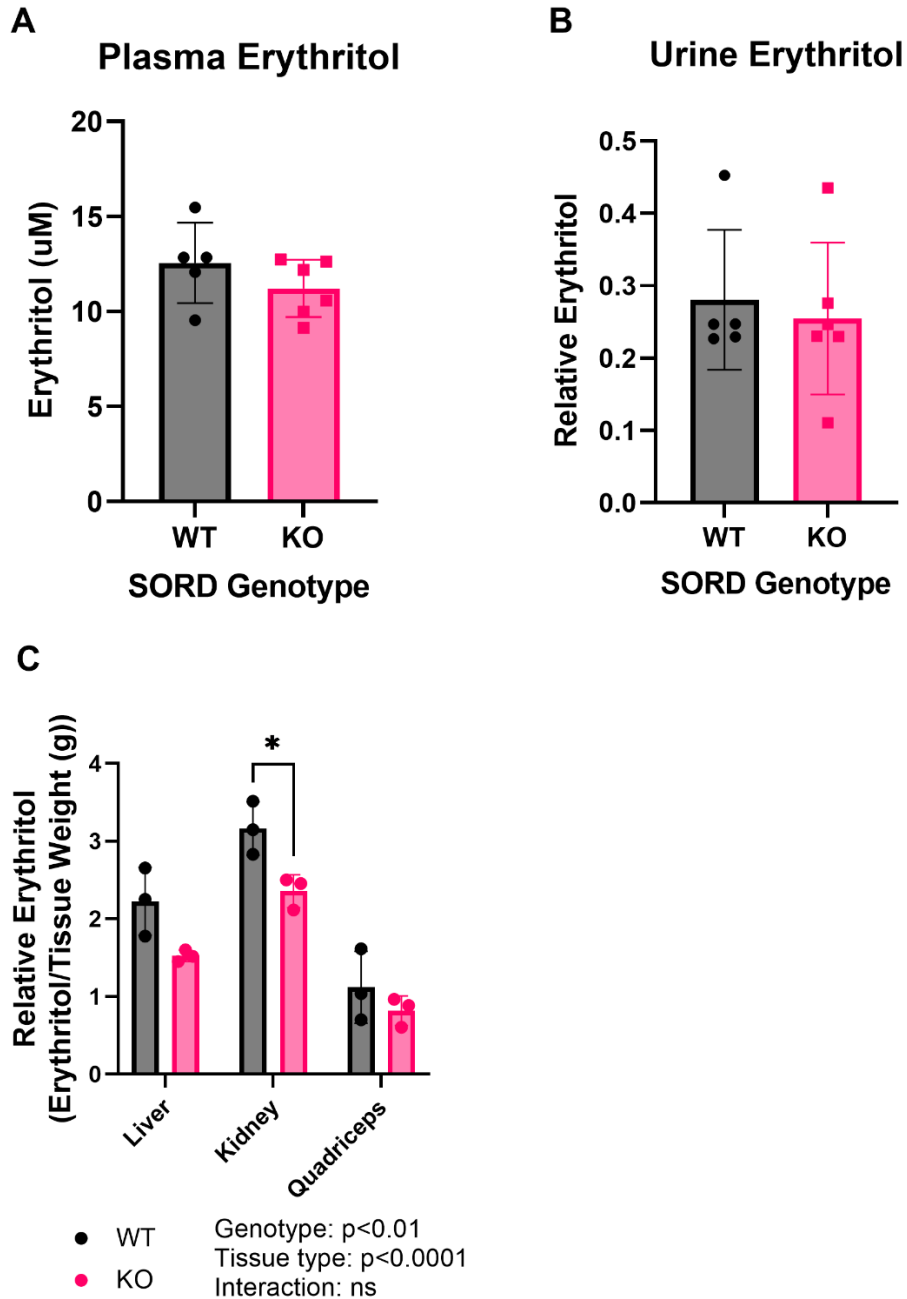
608 Erythritol was normalized to urinary creatinine content. Data are presented as mean \pm SD.

609 ** $p < 0.01$, *** $p < 0.001$, **** $p < 0.0001$. HFD: high-fat diet; LFD: low-fat diet.



610

611 **Figure 12. Sucrose significantly elevates erythritol in kidney and quadriceps.** Relative
612 erythritol content of A) liver, B) kidney, and C) quadriceps of mice following 8 weeks of dietary
613 treatment. Data are presented as mean \pm SD. **p<0.01, ***p<0.001. HFD: high-fat diet; LFD:
614 low-fat diet.



615

616 **Figure 13. SORD null animals have reduced tissue erythritol in response to sucrose**
617 **overfeeding.** A) Non-fasted plasma erythritol, B) relative urine erythritol, and C) relative tissue
618 erythritol in SORD WT and KO mice exposed to LFD with 30% sucrose. Data are presented as
619 mean \pm SD. * $p < 0.05$. KO: knockout; WT: wildtype.